

## Accepted Manuscript

The investigation of perpendicular anisotropy of ternary-alloy magnetic nanowire arrays using first-order-reversal-curve (FORC) diagrams

M. Arefpour, M. Almasi-Kashi, A. Ramazani, E. Golafshan

PII: S0925-8388(13)02056-2  
DOI: <http://dx.doi.org/10.1016/j.jallcom.2013.08.171>  
Reference: JALCOM 29306

To appear in:

Received Date: 24 July 2013  
Revised Date: 24 August 2013  
Accepted Date: 26 August 2013



Please cite this article as: M. Arefpour, M. Almasi-Kashi, A. Ramazani, E. Golafshan, The investigation of perpendicular anisotropy of ternary-alloy magnetic nanowire arrays using first-order-reversal-curve (FORC) diagrams, (2013), doi: <http://dx.doi.org/10.1016/j.jallcom.2013.08.171>

This is a PDF file of an unedited manuscript that has been accepted for publication. As a service to our customers we are providing this early version of the manuscript. The manuscript will undergo copyediting, typesetting, and review of the resulting proof before it is published in its final form. Please note that during the production process errors may be discovered which could affect the content, and all legal disclaimers that apply to the journal pertain.

# The investigation of perpendicular anisotropy of ternary-alloy magnetic nanowire arrays using first-order-reversal-curve (FORC) diagrams

M. Arefpour<sup>a,\*</sup>, M. Almasi-Kashi<sup>a,b</sup>, A. Ramazani<sup>a,b</sup>, E. Golafshan<sup>a</sup>

<sup>a</sup> Institute of Nanoscience and Nanotechnology, University of Kashan, Kashan, Iran

<sup>b</sup> Department of Physics, University of Kashan, Kashan, Iran

[mn.arefpoor@gmail.com](mailto:mn.arefpoor@gmail.com)

Tel.: +98 3615552935; fax: +98 3615552935.

## Abstract

FeCoZn nanowires with controlled diameters have been prepared using pulse electrochemical deposition in anodized aluminum oxide templates. The magnetic measurements revealed significant effect of annealing on the saturation magnetization ( $M_s$ ) and coercivity of nanowires. When the applied field was along the wire axis, the coercivity of as-deposited nanowires was found to be almost independent of diameter, while that of the annealed nanowires decreased with diameter. FORC diagrams of annealed sample with 80 nm diameter showed crossover of magnetic easy axis from parallel to perpendicular to the wires axis. The as-deposited nanowire arrays show uniform diameter along the whole lengths of nanowires. The X-ray diffraction analysis revealed the segregation of magnetic and nonmagnetic phases, i.e. two peaks corresponding to (110) FeCo and (101) Zn.

**Keywords:** Magnetic properties; FORC diagram; Perpendicular anisotropy; Pore-widening.

## 1. Introduction

Nanostructured materials have received considerable attention in recent years due to their interesting optical, chemical, electrical, mechanical and magnetic properties [1–6]. Magnetic nanowires have attracted many interests from both fundamental research and technological point of views. In fact, magnetic nanowires exhibit improved properties in comparison with their bulk counterparts and offer great potential applications such as magnetic recording media and sensors [7, 8]. In spite of bulk state of magnetic metals, large shape anisotropy of nanowires leads to their magnetically hard properties. To improve the hard magnetic properties, many researchers have studied the micromagnetic reversal process, dimension and annealing condition effects on the magnetic properties [9-13].

The fabrication of nanowires based on anodic aluminum oxide (AAO) templates is encouraged for perpendicular magnetic recording media [14-16]. Many researches on Co, Ni, Fe, FeCo, CoCu, CoPt, FeNi and CoZn nanowires electrochemical deposited into the AAO have been recently published [17-24].

The shape and magnetocrystalline anisotropies and the magnetostatic interaction are main sources to affect magnetic behavior of nanowires in various applications. In this paper, first order reversal curve (FORC) as an effective technique is used to study interacting and coercive field distributions of the samples exposed to magnetic field in parallel and perpendicular directions to wires axis. An experimental set of FORCs consists of many minor hysteresis loops. A FORC measurement is started by magnetically saturating the sample which exposed to a high enough magnetic field in the selective positive direction. Field's polarity is then changed and ramped down to top branch of the major hysteresis loop as reversal premature negative saturation

magnetization. This reversal point will be defined as  $H_r$ . The field is then reversed back to the positive direction and magnetization is recorded as a function of the applied and reversal field. This process is repeated until the interior of the major hysteresis loop mapped out as counter plot. The FORC diagram consists of the representation of the FORC distribution function as

$$\rho_{FORC}(H_r, H) = -\frac{1}{2} \frac{\partial^2 M(H_r, H)}{\partial H_r \partial H}$$

The critical field ( $H_c = (H - H_r)/2$ ) and the interaction field ( $H_u = (H + H_r)/2$ ) are the orthogonal axes of the FORC diagrams. The FORC diagrams can be used to recognize the presence of magnetostatic interactions and study magnetization behavior of a sample as a contribution of single-domain (SD), multi-domain (MD), pseudo-single-domain (PSD) and superparamagnetic (SP) grains [25-27].

FeCoZn nanowires were synthesized with various diameters by ac pulse electrochemical deposition and their magnetic properties were investigated by analyzing magnetization curves at room temperature. Also, the effect of annealing and Zn addition on microstructure and magnetic properties of the FeCoZn nanowires were investigated.

## 2. Experimental

The AAO templates have been prepared by the two-step anodization process. Highly pure aluminum foils of 0.3 mm thickness were electropolished in a 1:4 volume mixture of perchloric acid and ethanol. The foils were then anodized in 0.3 M oxalic acid solution at 17 °C for 10 h at 40 V. To remove the anodized layer, the anodized foils were immersed in a mixture of 0.2 M chromic and 0.5 M phosphoric acids at 60 °C for 10 h. Foils were re-anodized for 2 h by the

same conditions as the first step. To increase the pore diameter, prepared samples were widened in 0.3 M phosphoric acid at 30 °C for 6, 12, 24 and 30 min [28, 29]. Following the pore widening step, voltage was reduced systematically to promote thinning of the barrier layer. The voltage was initially reduced from 40 V by a rate of 0.06 V s<sup>-1</sup> to 20 V and then 0.03 V s<sup>-1</sup> to 12 V and ultimately anodization continued in the last voltage for 1 min in order to equilibrate the barrier layer. A typical top view AFM image of the as-deposited nanopore arrays which were obtained by the two-step anodization method is seen in Fig. 1. Hexagonally arranged nanopores with 30 nm diameter and 100 nm interpore distances are observed.

An ac-pulse electrochemical deposition technique was performed to deposit nanowires into the nanopores. A sine waveform with 18/18 V reduction/oxidation voltage was employed during the electrochemical deposition process. Reduction and oxidation times were 5 ms and the off-time between pulses was 200 ms. Also the lengths of wires are identical (~2.5 μm), by adjusting the electrochemical deposition time. A solution composed of CoSO<sub>4</sub>·7H<sub>2</sub>O (42 g/l), FeSO<sub>4</sub>·7H<sub>2</sub>O (26 g/l), ZnSO<sub>4</sub>·7H<sub>2</sub>O (23 g/l), H<sub>3</sub>BO<sub>3</sub> (40 g/l) and C<sub>6</sub>H<sub>5</sub>O<sub>6</sub> (1 g/l) was used as electrolyte. The pH value of the electrolyte solution was initially about 3.5, which increased to 4 by adding NaHCO<sub>3</sub>. The samples were then annealed at 580 °C in a mixture of 15% hydrogen and 85% argon gases for 30 min. The structure and composition of FeCoZn nanowire arrays were studied by X-ray diffraction (XRD) and electron dispersive spectroscopy (EDS). The magnetic measurements include hysteresis loops and FORC analysis, were conducted by vibrating sample magnetometer (VSM) at room temperature. Scanning electron microscopy (SEM) and atomic force microscopy (AFM) were employed to investigate the surface morphology of samples.

### 3. Results and discussion

Fig. 2 shows cross section SEM micrograph of FeCoZn nanowires embedded in AAO templates which have parallel nanoholes with no intercrossing. Furthermore, the pore diameter of as-deposited sample is about 30 nm (Fig. 2(a)), while it increases to 50 nm when the widening time increases up to 12 min.

The SEM micrographs show the released nanowires of almost 30 and 80 nm diameters which were prepared by the templates widened at 0 and 30 min, respectively (Fig. 3). According to table 1, due to widening process the pore diameters increase in the rate of 1.6 nm/min. It should be noted that interpore distance was not changed during the pore widening.

EDX measurements revealed that composition of  $\text{Fe}_{46}\text{Co}_{38}\text{Zn}_{16}$  nanowires is converted to  $\text{Fe}_{30}\text{Co}_{22}\text{Zn}_{48}$  with increasing diameter from 50 to 80 nm.

Fig. 4 shows variation of  $H_c^{\text{oop}}$  and  $H_c^{\text{ip}}$  of as-deposited and annealed samples with diameter. It should be noted that the out-of-plane and in-plane coercivities ( $H_c^{\text{oop}}$  and  $H_c^{\text{ip}}$ ) are related to the direction of applied magnetic field parallel and perpendicular to the wires axis, respectively. The  $H_c^{\text{oop}}$  of as-deposited samples is diameter in-dependent, while that of annealed samples decreases with diameter. In the both as-deposited and annealed samples the diameter has relatively no effect on the  $H_c^{\text{ip}}$ . In addition  $H_c^{\text{ip}}$  and  $H_c^{\text{oop}}$  increase with annealing up to 8 and ~4 times, respectively. Because of minimum perpendicular anisotropy of the sample with 80 nm diameter it is studied with more analysis (see Fig.4). The as-deposited and annealed in-plane and out-of-plane FORC diagrams of this sample are shown in Fig. 5. This nanowire composed of single domain particles with two phases. Soft phase correlated to counter plot is approached to

$H_u$  axis and relatively hard phase elongated in  $H_c$  direction. The out-of-plane FORC of as-deposited sample (Fig. 5(a)) indicates a very weak interacting system with low coercivity distribution, while the relatively non-interacting annealed sample shows a wide coercivity distribution (Fig. 5(b)). Same magnetic behavior in-plane and out-of-plane FORC diagrams of annealed sample (Figs 5(b) and (c)) is seen, but with relatively strong hard phase in in-plane FORC. The in-plane FORC of as-deposited sample is not measured, because of very weak coercivity and saturation magnetization which presents a noisy curve. FORC diagrams of "FeCoB" nanowires with 175 nm diameter is reported to elongate in  $H_u$  direction [27]. The hysteresis loops, also show weak magnetic properties of  $H_c^{oop}$ ,  $H_c^{ip}$  and  $M_s$  which improves after annealing (Fig. 6).

X-ray diffraction patterns of 80 nm diameter FeCoZn nanowire arrays embedded into the templates are presented in Fig. 7. In order to take only FeCoZn peaks into account, the following considerations were employed. The sample was located on an amorphous substrate. The aluminum was then removed from the rear of the samples using a mixture of HCl and saturated  $CuSO_4$ . It is seen that as-deposited sample has amorphous structure, or the crystal grains are so small to be detectable. Annealing procedure leads to segregate magnetic and non-magnetic grains in which a sharp (110) bcc FeCo peak and a weak (101) hcp Zn peak are attained. This phenomenon is also reported for FeCoPb nanowire arrays in which annealing leads to form FeCo (110) in bcc structure and enhancing the magnetic properties [30].

Due to existence of very fine magnetic grains the pore-widening has no significant effect on the magnetic properties of as-deposited nanowires (Fig. 4(a)) The XRD pattern in Fig. 5 indicates amorphous as-deposited nanowires. Two distinct crystalline magnetic FeCo and non-

magnetic Zn phases also appeared after annealing. Annealing treatment up to 580 °C (a temperature over melting point of bulk Zn, i.e. 420 °C) leads to form FeCo clusters and aggregate pinned Zn atoms in the FeCo grain boundaries [31]. This explanation has been achieved regarding to the XRD and FORC analyzes (see Figs. 5 and 6). In fact, there are very small amorphous FeCoZn particles into as-deposited nanowires, while annealing causes magnetic FeCo clusters placed in the bed of Zn.

As mentioned before, although  $H_c^{ip}$  is independent on the wires diameter, the ratio of  $H_c^{oop}/H_c^{ip}$  of annealed nanowires is less than that of as-deposited one. In addition, the similarity of in-plane and out-of-plane FORC diagrams (Figs 6(b) and (c)), emphasizes low perpendicular anisotropy of annealed samples which tend to be disappeared. After pore-widening, relatively spherical FeCo clusters with various sizes distributed between Zn atoms minimize the shape anisotropy thereby easily magnetize in both parallel and perpendicular direction of applied field leads to obtain an almost equal  $H_c^{oop}$  and  $H_c^{ip}$ . Wide distribution of FeCo grains size (with maximum pore diameter size) causes to vary the coercivity in a wide range (from a few Oe up to 3 KOe (see Fig. 5(b) and (c))). As reported in our previous work [26]  $H_c^{oop}$  of FeCo nanowires reduce with diameter.

The reversal magnetization in as-deposited nanowires was expected to follow the coherent model which is related to single domain particles, in which the behavior of  $H_c^{oop}$  is independent of the particle's size. But it obeys the curling mode in which  $H_c^{oop}$  decreases by increase in diameter.

The influence of pore-widening on the saturation magnetization ( $M_s$ ) of nanowires is shown in Fig. 8(a). Reduction of  $M_s$  with diameter is assigned to more deposition of Zn ions into

the wider pores during electrochemical deposition process. According to anomalous co-deposition, more deposition of element with less positive standard electrode potential is expected [32]. Since electrolyte concentration is the same, increasing of anomalous deposition with diameter is then not far from expectation. The Slater–Pauling curve predicts the spontaneous magnetization of bulk FeCo alloy increases with Co content [33]. Therefore, the  $M_s$  of FeCoZn nanowires reduces with diameter, decreasing the Co content, by increasing the diameter due to decrease of spontaneous magnetization which is clearly seen in Fig 8(b). Improvement of  $M_s$  of annealed samples arises from relieving of internal stress and defects produced by rapid deposition in as-deposited nanowires [10] and segregation of magnetic and non-magnetic phases as discussed before.

#### 4. Conclusion

FeCoZn nanowire arrays were fabricated by ac pulse electrochemical deposition into the porous alumina prepared by the two-step anodization method. Amorphous structure of as-deposited nanowires crystallized to distinct FeCo and non-magnetic Zn phases after annealing. The higher coercivity of the annealed samples may be associated with segregation of FeCo grains by non-magnetic Zn atoms and pinning of solidified Zn particles. The  $H_c^{oop} / H_c^{ip}$  ratio indicated the easy axis along and perpendicular to as-deposited and annealed nanowires, respectively. FORC diagrams showed formation of single domain nanowires with wide coercivity distribution after annealing. The similarity of in-plane and out-of-plane FORC diagrams of annealed sample indicated low perpendicular anisotropy.

**References**

- [1] M. Law, J. Goldberger, P. Yang, *Annu. Rev. Mater. Res.* 34 (2004) 83.
- [2] C.R. Martin, L.A. Baker, *Science*. 309 (2005) 67.
- [3] Y. Rheem, B.Y. Yoo, W.P. Beyermann, N.V. Myung, *Nanotechnology*. 18 (2007) 125204.
- [4] J.M. Garcia-Martin, A. Thiaville, J. Miltat, T. Okuna, L. Vila, L. Piraux, *J.Phys. D: Appl. Phys.* 37 (2004) 965.
- [5] A.S. Samardak, E.V. Sukovatitsina, A.V. Ognev, L.A. Chebotkevich, R. Mahmoodi, S.M. Peighambari, M.G. Hosseini, F. Nasirpouri, *J. Phys: Conference Series*. 345 (2012) 012011.
- [6] D.A. Genov, A.K. Sarychev, M. Shalaev, A. Wei, *Nano. Lett.* 4(1) (2004) 153.
- [7] N. Zabala, M.J. Puska, R.M. Nieminen, *Phys. Rev. Lett.* 80 (1998) 3336.
- [8] M. Almasi Kashi, A. Ramazani, H. Abbasian, A. Khayyatian, *Sensors and Actuators A: physics*. 174 (2012) 69.
- [9] R. Lavín, C. Gallardo, J.L. Palma, J. Escrig, J.C. Denardin, *J. Magn. Magn. Mater.* 324 (2012) 2360.
- [10] X. Lin, G. Ji , T. Gao, X. Chang, Y. Liu, H. Zhang, Y. Du, *Solid. State. Commun.* 151 (2011) 1708.
- [11] K. Maaz, S. Karim, M. Usman, A. Mumtaz, J. Liu, J.L. Duan, M. Maqbool, *Nanoscale. Res. Lett.* 5 (2010) 1111.

- [12] R. Lavin, J.C. Denardin, A.P. Espejo, A. Cortés, H. Gómez, J. Appl. Phys. 107 (2010) 09B504.
- [13] S.L. Lim, F. Xu, N.N. Phuoc, C.K. Ong, J. Alloys. Compd. 505 (2010) 609.
- [14] H.J. Richter, J. Phys. D: Appl. Phys. 40 (2007) R149.
- [15] R.M. White, R.M.H. New, R.F.W. Pease, IEEE Trans. Magn. 33 (1996) 990.
- [16] T. Thurn-Albrecht, J. Schotter, G.A. Kastle, N. Emley, T. Shibauchi, L. Krusin-Elbaum, K. Guarini, C.T. Black, M.T. Tuominen, T.P. Russell, Science. 290 (2000) 2126.
- [17] S. Shingubara, K. Morimoto, M. Nagayanagi, T. Shimizu, O. Yaegashi, G.R. Wu, H. Sakaue, T. Takahagi, K. Takase, J. Magn. Magn. 272–276 (2004) 1598.
- [18] S. Karim, K. Maaz, Mater. Chem. Phys. 130 (2011) 1103.
- [19] J.B. Wang, Q.F. Liu, D.h. Xue, F.h. Li, Chin. Phys. Lett. 21 (2004) 945.
- [20] H.l. Sua, S.L. Tang, R.l. Wang, Y.q. Chen, C. Jia, Y.W. Du, Chin. J. Chem. Phys. 22 (2002) 82.
- [21] Z. Zhang, Q. Wu, K. Zhong, S. Yang, X. Lin, Z. Huang, J. Magn. Magn. Mater. 303 (2006) e304.
- [22] S.K. Lim, G.H. Jeong, I.S. Park, S.M. Na, S.J. Suh, J. Magn. Magn. Mater. 310 (2007) e841.
- [23] Q.F. Liu, C.X. Gao, J.J. Xiao, D.S. Xue, J. Magn. Magn. Mater. 260 (2003) 151.

- [24] M. Koohbor, S. Soltanian, M. Najafi, P. Servati, *Mater. Chem. Phys.* 131 (2012) 728.
- [25] I.D. Mayergoyz, *IEEE Trans. Magn.* 22 (1986) 603.
- [26] S. Alikhazadeh-Arani, M. Almasi-Kashi, A. Ramazani, *Current. Appl. Phys.* 13 (2013) 664
- [27] F. Béron, L. Clime, M. Ciureanu, D. Ménard, R.W. Cochrane, A. Yelon, *IEEE Trans. Magn.* 42 (2006) 3060.
- [28] H.M. Yu, J. Lee, *Current. Appl. Phys.* 11 (2011) S339.
- [29] D.H. Choi, P.S. Lee, W. Hwang, K.H. Lee, H.C. Park, *Current. Appl. Phys.* 6S1 (2006) e125.
- [30] R.L. Wang, S.L. Tang, Y.G. Shi, X.L. Fei, B. Nie, Y.W. Du, *J. Appl. Phys.* 103 (2008) 07D507.
- [31] G.B. Ji, W. Chen, S.L. Tang, B.X. Gu, Z. Li, Y.W. Du, *Solid. State. Commun.* 130 (2004) 541.
- [32] A. Brenner, Academic Press, New York and London. 2 (1963) 221.
- [33] J.C. Slater, *J. Appl. Phys.* 8 (1937) 385.

**Figure captions**

Fig. 1. A typical top view AFM image of the as-deposited nanopore arrays obtained by the two step anodization method.

Fig. 2. Cross section SEM micrograph of nanoporous arrays prepared at (a) 0 and (b) 12 min pore widening times.

Fig. 3. SEM micrographs of released nanowires from AAO templates, widened at (a) 0 and (b) 30 min.

Fig. 4. The out-of-plane and in-plane coercivity of (a) as-deposited and (b) annealed nanowire arrays as a function of diameter.

Fig. 5. The out-of-plane FORC diagrams of (a) as-deposited, (b) annealed nanowires with 80 nm diameter and (c) in-plane FORC diagram of the annealed sample.

Fig. 6. Out-of-plane and in-plane hysteresis loops of (a) as-deposited and (b) annealed nanowire arrays with 80 nm pore diameters.

Fig. 7. X-ray diffraction patterns of as-deposited and annealed FeCoZn nanowires with 80 nm pore diameter.

Fig. 8. (a) The saturation magnetization of as-deposited and annealed nanowire arrays as a function of diameter. (b) Out-of-plane hysteresis loops of the annealed nanowire arrays with different pore diameters.

**Table 1:** The correlation of widening time and pore diameter.

Widening time	0	6	12	24	30
(min)					
Diameter (nm)	30	40	50	60	80

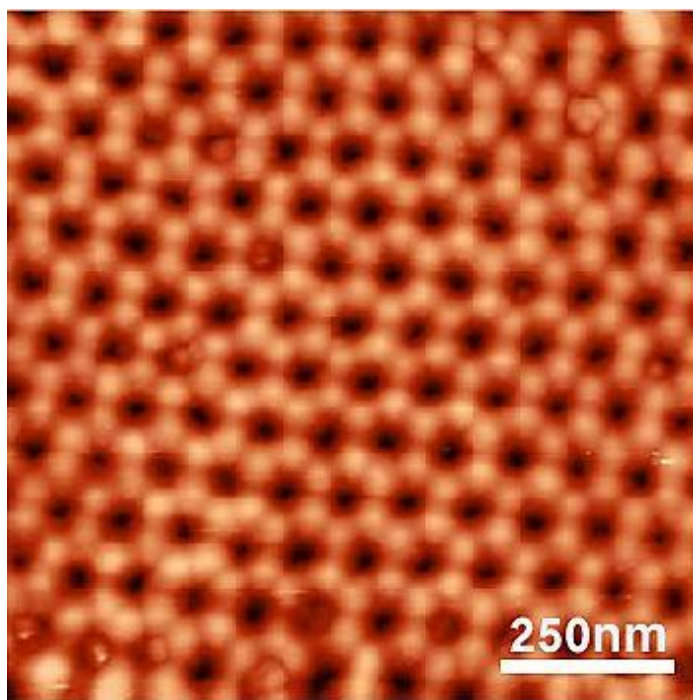


Fig. 1

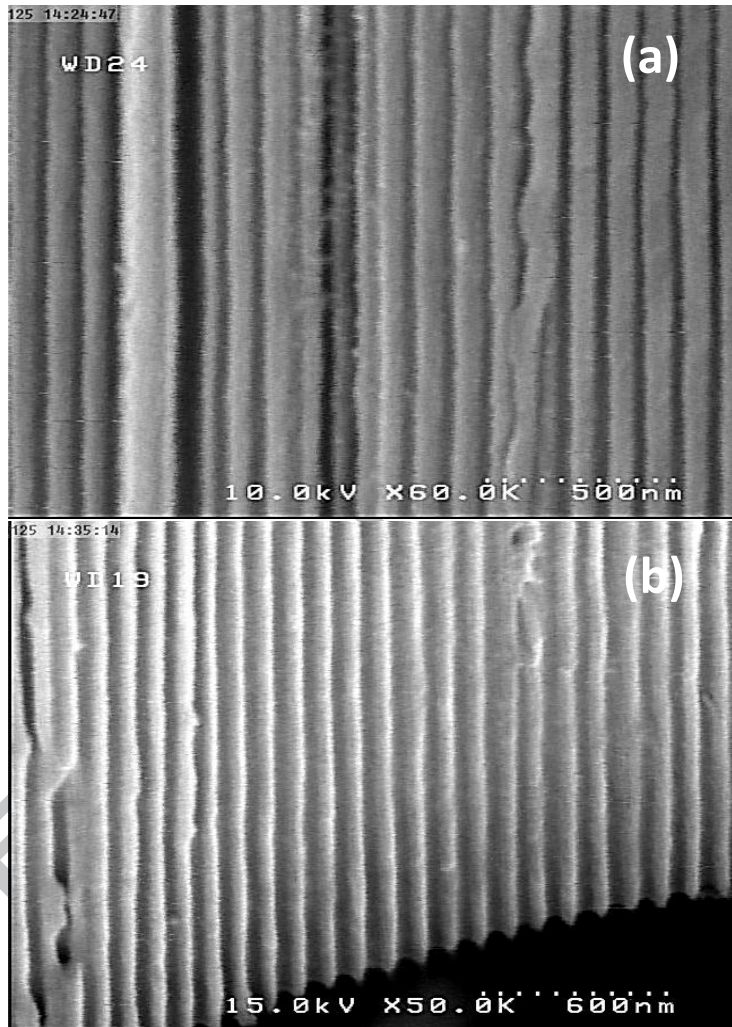


Fig. 2

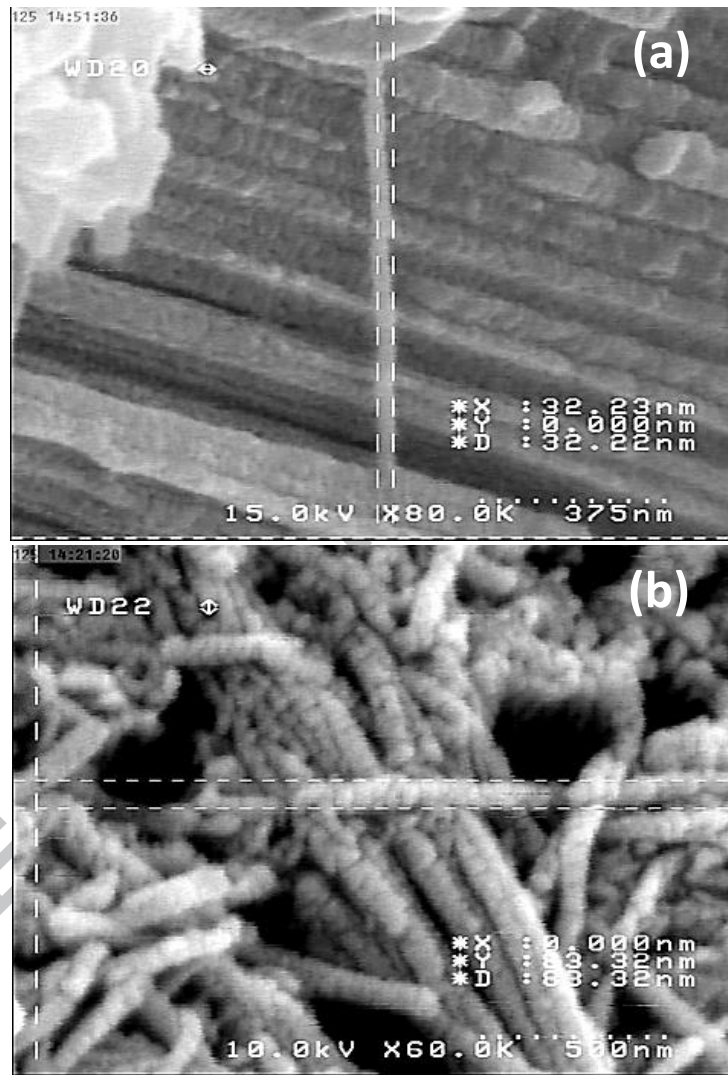


Fig. 3

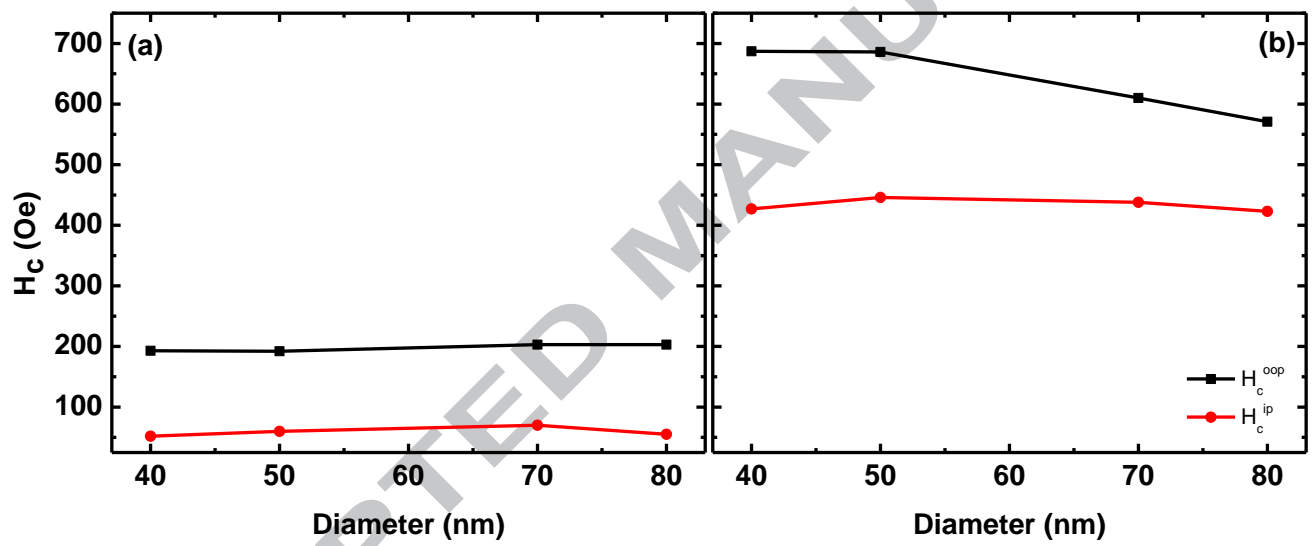
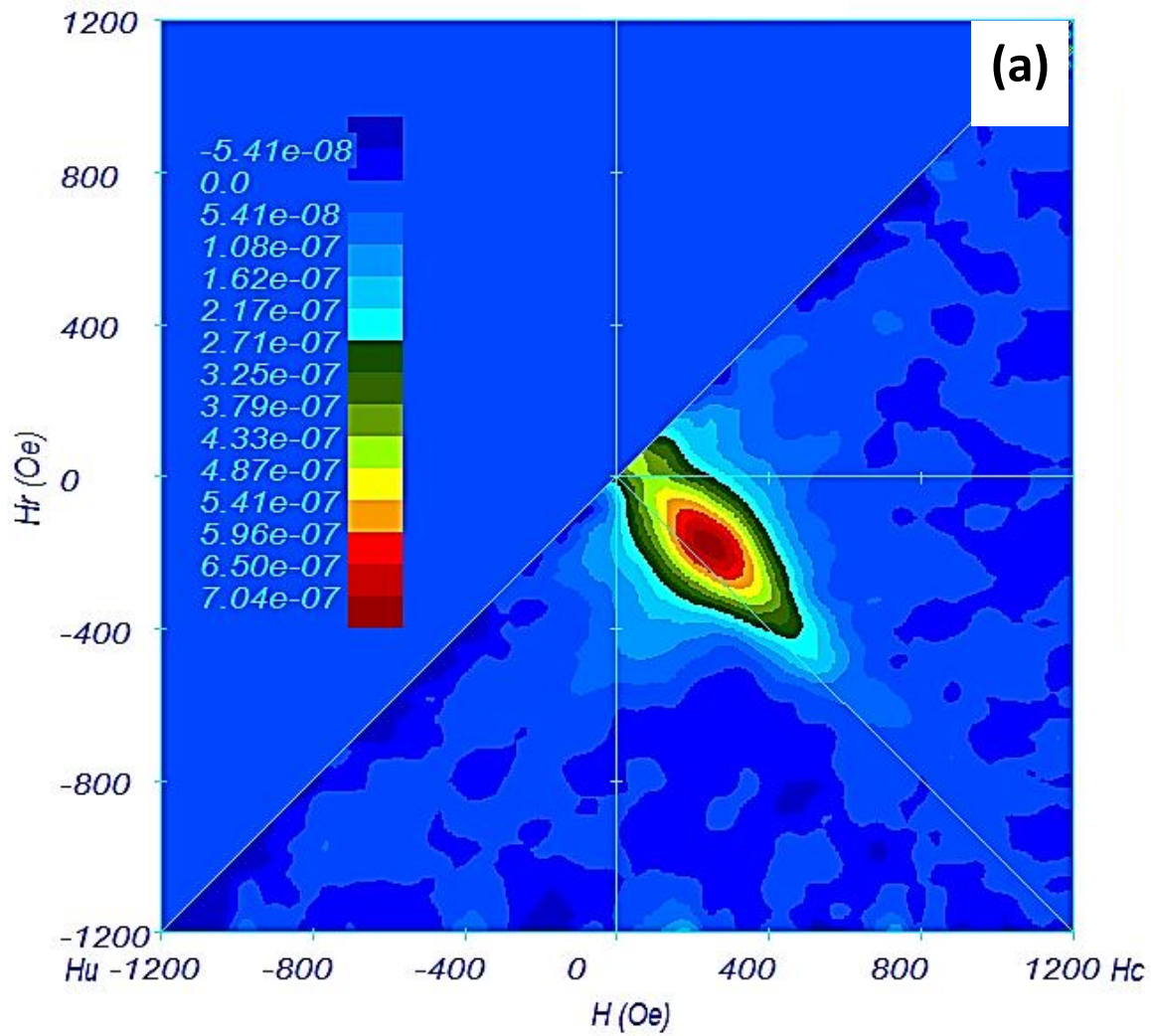
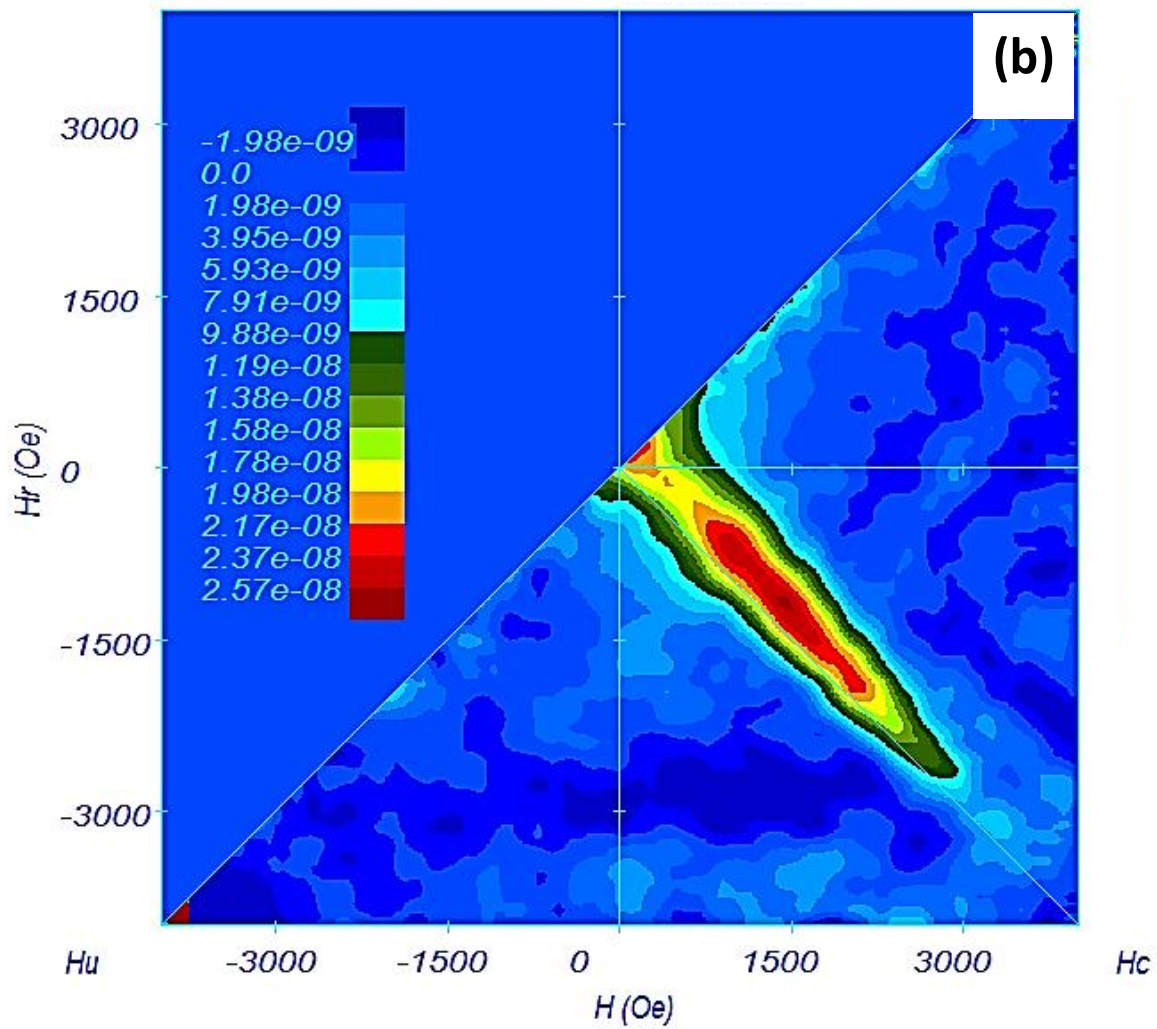


Fig. 4

DT





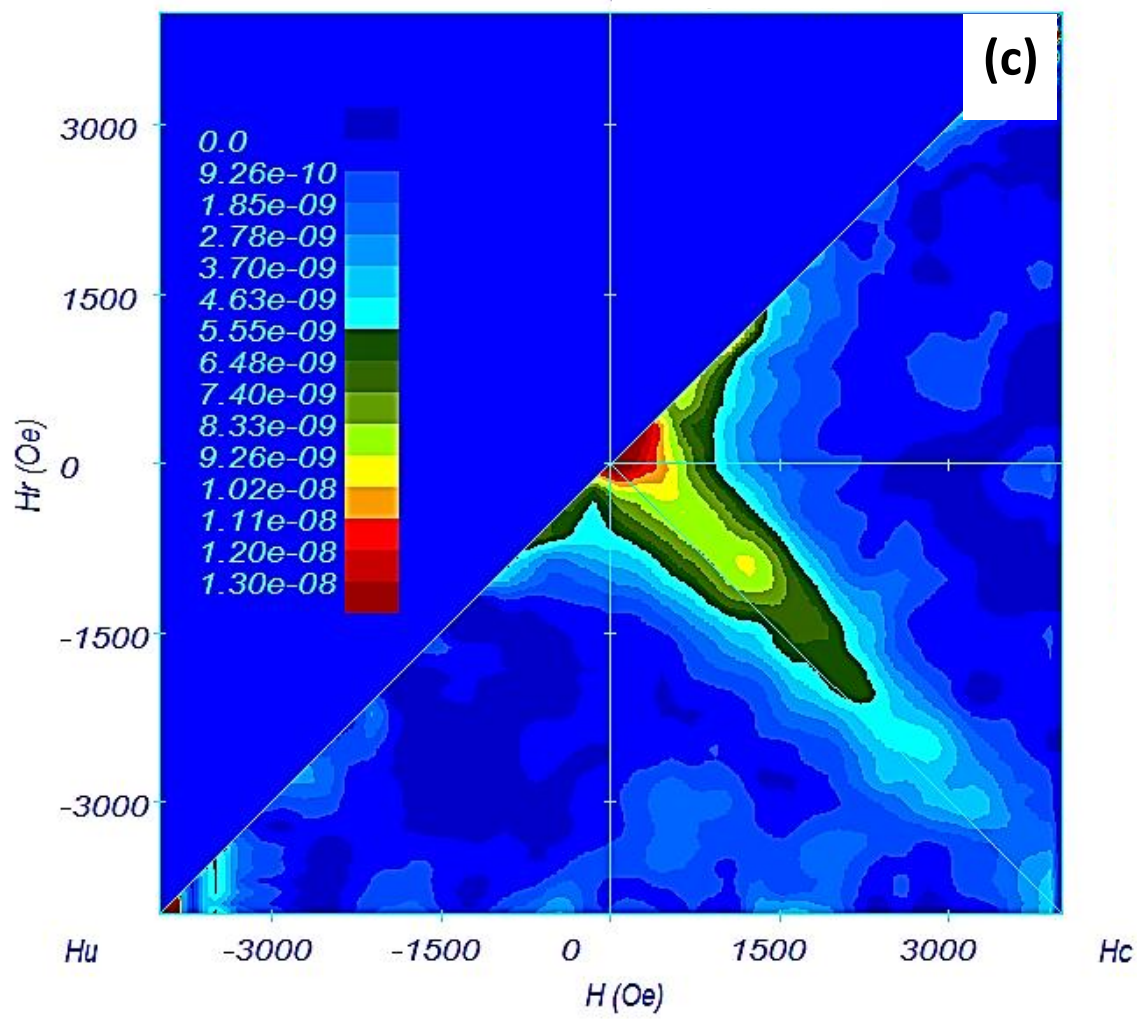


Fig. 5

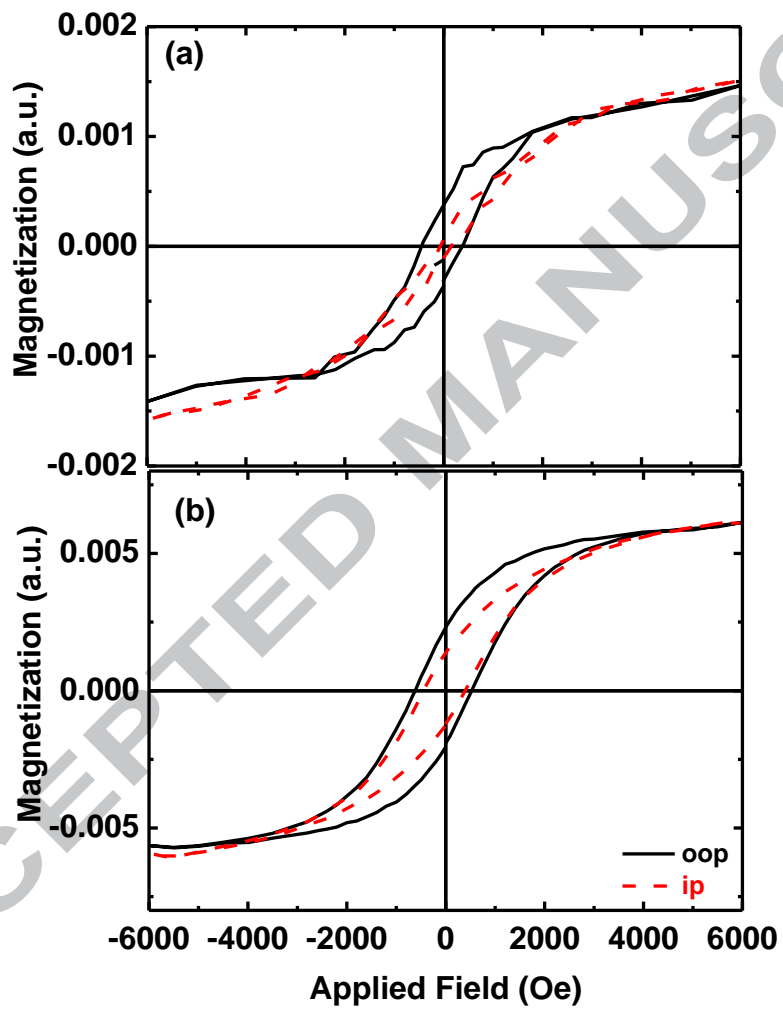


Fig. 6

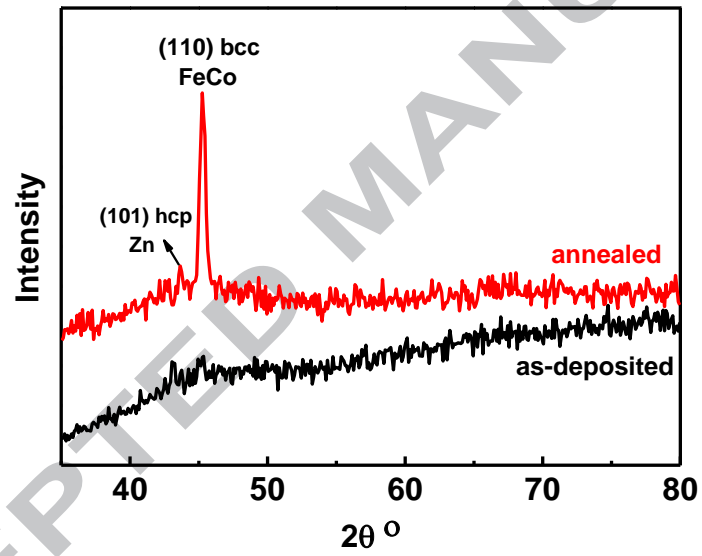


Fig. 7

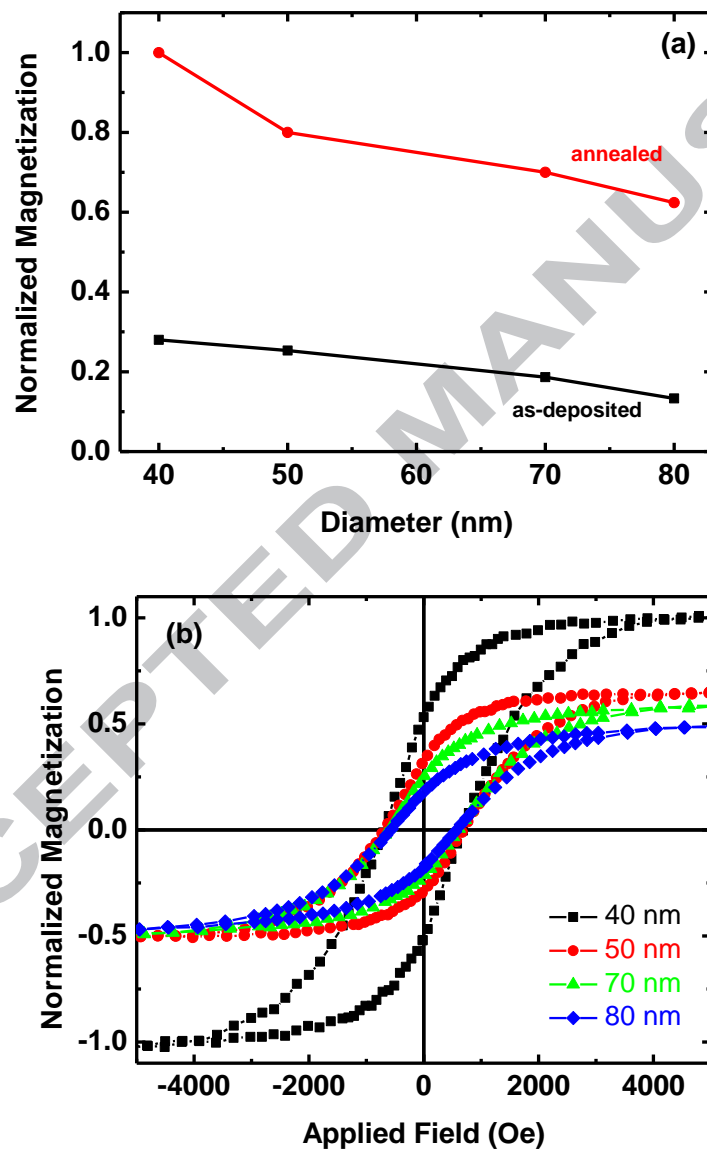


Fig. 8

FeCoZn NWs were fabricated by electrochemical deposition with various diameters.

Easy axis is along and perpendicular to as-deposited and annealed NWs, respectively.

FORC diagrams showed that NWs composed of single domain particles with two phases.

ACCEPTED MANUSCRIPT